

# Magnetic and electrochemical properties of nickel oxide microstructures prepared by hydrothermal method

N Boonraksa<sup>1</sup>, S Maensiri<sup>2</sup>, E Swatsitang<sup>3</sup> and K Wongsaprom<sup>1,\*</sup>

<sup>1</sup>Department of Physics, Faculty of Science, Maharakham University, Maharakham, 44150, Thailand

<sup>2</sup>School of Physics, Institute of Science, Suranaree University of Technology, Nakhon Ratchasima, 30000, Thailand

<sup>3</sup> Institute of Nanomaterials Research and Innovation for Energy (IN-RIE), NANOTEC-KKU RNN on Nanomaterials Research and Innovation for Energy, Khon Kaen University, Khon Kaen, 40002, Thailand

\*E-mail: kwanruthai.w@msu.ac.th

**Abstract.** Nickel oxide microstructures were successfully synthesized by hydrothermal method. The structure, morphology, surface and porosity of the NiO hexagonal plates indicated the formation of NiO without appearing any secondary phases, occupying the typical cubic structure. The ferromagnetic behaviour was examined by vibrating sample magnetometer (VSM). The sample exhibited ferromagnetic behaviour at room-temperature with the magnetic moment value of  $\sim 160$  memu/g. The cyclic voltammetry (CV) and galvanostatic charge-discharge (GCD) analysis were used to examine the electrochemical capacitance of the sample. The specific capacitance of the sample at a current density of 1 A/g was obtained to be 174.14 F/g. The cycle stability was excellent usability 76.6% after 500 cycles at a current density of 5 A/g.

## 1. Introduction

Transition metal oxides ( $\text{MnO}_2$ ,  $\text{Co}_3\text{O}_4$ ,  $\text{ZnO}_2$ , NiO, etc.) are the most important active electrode materials for supercapacitors, where highly reversible redox processes are involved at the surface area [1-4]. Among these metal oxides, NiO is very popular due to its ferromagnetic behaviour above 523 K and it is an intrinsic p-type semiconductor ( $E_g \approx 3.6 - 4.0$  eV) [5]. Apart from the magnetic properties, NiO has been considerable interest in the electrochemical properties. It has very good chemical, high thermal stability and a very high theoretical specific capacitance [6-10]. The electrochemical performance and magnetic properties of NiO have been studied by Ahmad *et al.* [11]. Electrochemical studies suggest the redox nature of this material with a strong pseudo capacitance with the specific capacitance of 210 F/g at scan rate of 100 mV/s. Vyas *et al.* [12] reported the magnetic properties of NiO with a value of magnetization of about 0.22 emu/g and a specific capacitance of 123.6 F/g at a scan rate of 10 mV/s.

In this paper, we study the magnetic and electrochemical performance of NiO microstructures synthesized by hydrothermal method. The structural analysis of NiO microstructures was employed X-ray diffraction (XRD). The morphology of the sample was observed by field emission scanning electron microscopy (FE-SEM). The chemical composition of the sample was investigated by energy dispersive X-ray spectroscopy (EDS). The porous nature of NiO microstructure was analysed using a Brunauer-Emmett-Teller (BET) analyser. The magnetization was performed using vibrating sample

magnetometer (VSM) at 300 K. The electrochemical performance of materials was examined by cyclic voltammetry (CV) and galvanostatic charge-discharge (GCD).

## 2. Experimental procedure

In this work, nickel oxide microstructure was prepared by hydrothermal method. Nickel nitrate [ $\text{Ni}(\text{NO}_3)_2 \cdot 6\text{H}_2\text{O}$ , 0.1 M] was used as a precursor. Nickel nitrate was dissolved and stirred in 50 mL of deionized water (DI water) at room-temperature, followed by addition to ammonia solution until its pH reached 9. The green solution was changed to a Teflon-lined stainless-steel autoclave with heating treatment at 180 °C for 24 h. The green precipitates were picked by centrifugation and washed many times with DI water and ethanol separately, then dried the green powder at 70 °C for 24 h. Finally, the dried sample was calcined at 300 °C for 3 h. The crystal structure of the NiO microstructure was analysed by XRD (Bruker-D8 advanced X-ray diffractometer). FE-SEM and EDS were used to observe the morphology and elemental composition. The pore size analysis of the sample were calculated from nitrogen adsorption-desorption isotherm by using a BET analyser. The magnetic behaviour was characterised by VSM (Versa Lab VSM, Quantum Design). The electrochemical properties were examined by CV and GCD.

## 3. Results and discussion

The crystal structure of the NiO sample was primary examined by XRD. Figure 1 reveals the XRD pattern of NiO sample prepared by hydrothermal method. The diffraction peaks observed for the sample can be indexed to the pure phase of cubic structure (JCPDS No.47-1049). In addition, these narrow and high intensity diffraction peaks indicate the good crystallinity of the sample. Figure 2 reveals the spectrum of EDS for NiO microstructures. The spectrum reveals peaks of Ni and O. No evidence of any impurity phase was identified by XRD and EDS. Moreover, the presence of C, Cu and Au came from carbon tape, copper stub and Au coating on the surface of sample, respectively. The detailed morphology of NiO microstructures was studied by FE-SEM (inset in figure 2). The FE-SEM image reveals the large hexagonal plates with some fractures due to the calcination at high temperature [13, 14]. The average crystallite size is about  $787 \pm 54$  nm.

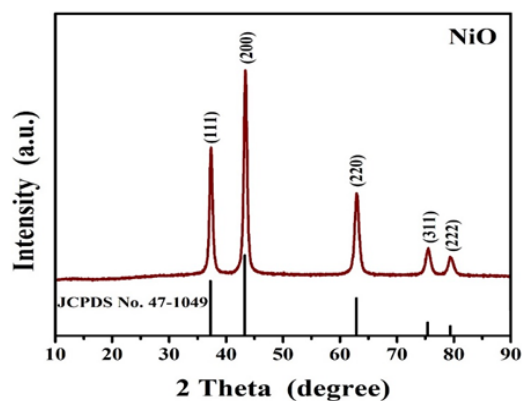


**Figure 1.** The pattern of XRD for NiO sample.

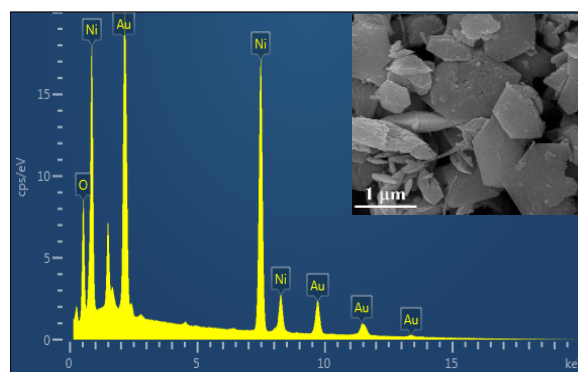


**Figure 2.** EDS spectrum of the sample, with inset showing its FE-SEM image.

The electrochemical properties of NiO microstructures were investigated by CV and GCD analysis. Figure 3(a) presents the cyclic voltammograms at 2, 5, 10, 20, 50, 100 and 200 mV/s in 6 M of KOH, revealing the interesting electrochemical behavior in the voltage range 0.0 – 0.55 V. The CV curves show pseudocapacitive behavior with the anodic peak appearing at 0.36 to 0.46 V, indicating the oxidation process of NiO to NiOOH. The reduction process of the reversible redox-reaction type are observed at 0.12 to 0.25 of the cathodic peak. The first process is suggested to be the adsorption and desorption of  $\text{OH}^-$  ions on the NiO surface structure, occurring near the interface of electrolyte and electrode [15], according to the equation (1). The second one is the intercalation/deintercalation of Ni ions due to the reversible redox-reaction of  $\text{Ni}^{2+}/\text{Ni}^{3+}$  as presented in equation (2).

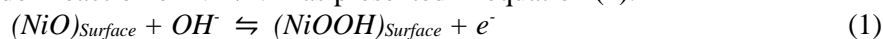
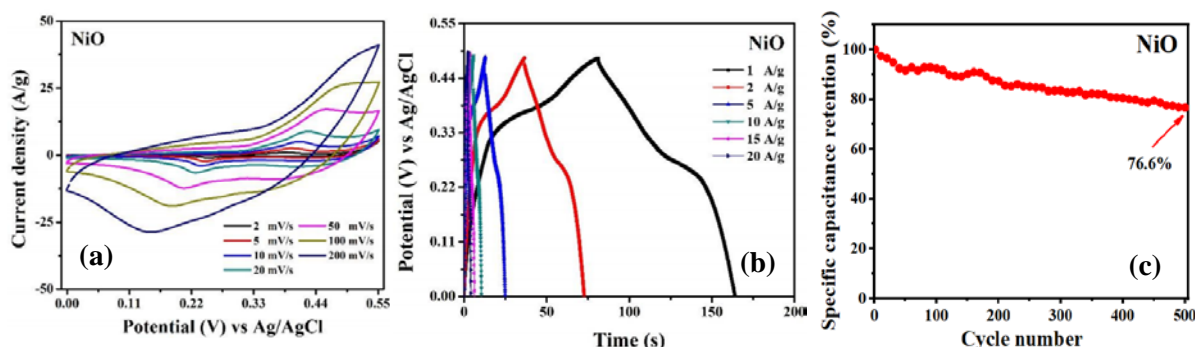
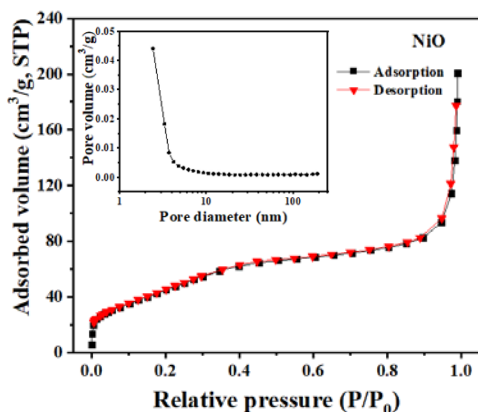


Figure 3(b) reveals the GCD curves at different current densities (1, 2, 5, 10, 15, 20 A/g). The GCD curves exhibit the two levels of discharge, as a result of the change in the oxidation number of NiO/NiOOH due to the reversible redox-reaction, indicating the pseudocapacitive behavior [16]. The determined specific capacitance of the sample is a value of 174.14 F/g at the current density of 1 A/g. This value is less than theoretical capacitance [6], due to the low surface area with low active sites in our sample. The sample exhibits an excellent retention in discharge-charge test by 76.6% cycle after 500 cycles as presented in figure 3(c).



**Figure 3.** (a) CV curves of NiO microstructures, (b) GCD curves of NiO sample and (c) The capacitance retention of the sample.



**Figure 4.** The nitrogen adsorption-desorption analysis with inset showing the pore size distribution.

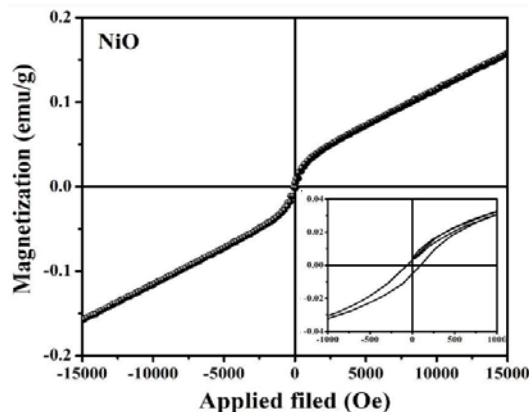


**Figure 5.** M-H curve of the NiO sample at room-temperature.

The porous nature is investigated by nitrogen adsorption-desorption. The nitrogen adsorption-desorption result, with revealed the Type-II of typical microporous material. Figure 4 reveals the specific surface area of the sample is 176.46 m<sup>2</sup>/g, which calculated by BET. The calculation of pore size distribution was studied by the BJH (Barrett-Joyner-Halenda) method [inset in figure 4]. The NiO sample has the average pore size and pore volume of 2.43 nm and 0.11 cm<sup>3</sup>/g, respectively. This result of the examining the surface area confirms the specific capacity of the material. Although the NiO has a high specific surface area caused by the calcination process, it yields a low specific capacitance. This might be result from the low average pore size and pore volume.

Figure 5 reveals the magnetization curve of the NiO sample at room-temperature. NiO microstructure shows weak ferromagnetic behaviour with a magnetization around 160 memu/g and coercivity of 80.6 Oe at the applied magnetic field of 15 kOe. A weak ferromagnetic behaviour of the sample, could result from the structural defects that formed an oxygen gap from thermal processes causing bound magnetic polaron (BMP) interactions [17, 18]. This result is consistent with the report of Bharathy and Raji [19],

studying the effects of Co doping in NiO. The author found that the pure NiO and Co-doped NiO exhibited a weak ferromagnetic behaviour, causing by the oxygen gap defect with electron lone pair confined to it. Therefore, the occurred polarization could result in a weak ferromagnetism at room-temperature. Moreover, our work also consistent with the research of Suresh *et al.* [20] revealing the evidence of superparamagnetism and weak ferromagnetism in NiO nanoflakes.

#### 4. Conclusion

Microstructures of NiO were synthesized by a hydrothermal method. The average crystalline size of the obtained product is about  $787 \pm 54$  nm. The NiO microstructure exhibited a good specific capacitance (174.14 F/g) and a high cycle stability (76.6% capacitance retention after 500 cycles). The magnetic measurement showed the weak ferromagnetic behaviour of the NiO microstructure with magnetization of approximately 160 memu/g and coercivity of 80.6 Oe at the applied magnetic field of 15 kOe. The authors expect this study to further advance the basic knowledge for electrode and magnetic materials.

#### Acknowledgments

The authors would like to thank the center of excellence in advanced functional materials, Suranaree University of Technology, Thailand for CV and GCD facilities. This work was financially supported by Thailand Science Research and Innovation (TSRI) 2021.

#### References

- [1] Li F, Xing Y, Huang M, Li K L, Yu T, Zhang Y X and Losic D 2015 *J. Mater. Chem. A* **3** 7855
- [2] Wang Y, Lei Y, Li J, Gu L, Yuan H and Xia D 2014 *ASC Appl. Mater. Interfaces* **6** 6739
- [3] Xiao X, Han B, Chen G, Wang L and Wang Y 2017 *Sci. Rep.* **7** 40167
- [4] Khairy M and El-Safty S A 2013 *RSC Adv.* **3** 23801
- [5] Din M I and Rani A 2016 *Int. J. Anal. Chem.* **2016** 3512145
- [6] Chen J, Huang Y, Li C, Chen X and Zhang X 2016 *Appl. Surf. Sci.* **360** 543
- [7] Li X, Xiong S, Li J, Bai J and Qian Y 2012 *J. Mater. Chem.* **22** 14276
- [8] Ding S, Zhu T, Chen J S, Wang Z, Yuan C and Lou X W 2011 *J. Mater. Chem.* **21** 6602
- [9] Yuan Y F, Xia X H, Wu J B, Yang J L, Chen Y B and Guo S Y 2010 *Electrochem. Commun.* **12** 890
- [10] Song X and Gao L 2008 *J. Phys. Chem. C* **112** 15299
- [11] Ahmad T, Ramanujachary K V, Lofland S E and Ganguli A K 2006 *Solid State Sci.* **8** 425
- [12] Vyas R, Navin K, Tripathi G K and Kurchania R 2021 *Optik* **231** 166433
- [13] Nathan T, Aziz A, Noor A F and Prabakaran S R S 2008 *J. Solid State Electrochem.* **12** 1003
- [14] Liu X M, Zhang X G and Fu S Y 2006 *Mater. Res. Bull.* **41** 620
- [15] Zhang L, Chen Q, Han X and Zhang Q 2018 *J. Clust. Sci.* **29** 1089
- [16] Kong D S, Wang J M, Shao H B, Zhang J Q and Cao C N 2011 *J. Alloys Compd.* **509** 5611
- [17] Schuele W J and Deetscreek V D 1962 *J. Appl. Phys.* **33** 1136
- [18] Bi H, Li S, Zhang Y and Du Y 2004 *J. Magn. Magn. Mater.* **277** 363
- [19] Bharathy G and Raji P 2018 *Physica B: Condens. Matter* **530** 75
- [20] Suresh R, Ponnuswamy V, Sankar C, Maniekam M, Venkatesan S and Perumal S 2017 *J. Magn. Magn. Mater.* **411** 787